Fouling Characteristics of Dissolved Organic Matter in Papermaking Process Water on Polyethersulfone Ultrafiltration Membranes

Wenpeng Su, Chen Chen, Yulian Zhu, Weisheng Yang, and Hongqi Dai*

In the papermaking industry, closure of process water (whitewater) circuits has been used to reduce fresh water consumption. Membrane separation technology has potential for use in treating process water for recirculation. The purpose of this study was to reveal the fouling characteristics of a polyethersulfone (PES) ultrafiltration membrane caused by dissolved organic matter (DOM) in process water. Ultrafiltration membranes (UF) and DAX ion exchange resins were applied to characterize the molecular weight (MW) and hydrophilicity distribution of DOM. The interactions between various fractions of DOM and a PES ultrafiltration membrane were investigated. The membrane fouling characteristics were elucidated by examining the filtration resistances and linearized Herman's blocking models. The results demonstrated that the membrane was fouled significantly by much of the MW distribution. The membrane was fouled more significantly by the low MW fraction rather than the high MW fraction. The filtration resistances and the fitted equation of Hermia's laws indicated that hydrophilic organics were the main foulants. The hydrophilic organics partially block the membrane pores and form intermediate blocking, reducing the effective filtration area, while the hydrophobic organics form a gel layer or cake on the surface of the membrane.

INTRODUCTION

In recent years, the closure of process water circuits in the papermaking industry has been implemented to reduce effluent discharge and fresh water consumption to comply with stringent environmental regulations (Natalia *et al.* 2013). However, the accumulation of dissolved organic matter (DOM) in process water, such as carbohydrates, lipophilic extractives, and other chemicals, interferes with the process of papermaking and degrades the quality of the production process (Chen *et al.* 2011; Wu *et al.* 2014a). To solve such problems, methods including flocculation (Stevenson 1990), bio-treatment (Huuhilo *et al.* 2002), adsorption (Wu *et al.* 2014b), and membrane filtration (Wu *et al.* 2009) have been developed to remove dissolved organics. Membrane filtration has been established as an advanced method to reduce or recover organics from process water. Membrane separation usage has increased rapidly in the past few decades on account of its advantages (compact module and small footprint) over conventional treatments.

However, membrane fouling caused by the foulants in whitewater has imposed a serious constraint for employing membrane technology in the water treatment field, especially in the papermaking industry (Rocas *et al.* 2014). The progressive decline of

bioresources.com

membrane flux reduces membrane permeability and filtration efficiency (Choi *et al.* 2013). Numerous studies have focused on the effects of interfacial characteristics, including pollutant size, surface hydrophobicity, and charge, on membrane fouling (Carroll *et al.* 2000; Kilduff and Mattaraj 2004; Lowe and Hossain 2008; Vela and Blanco 2008; Lee *et al.* 2009). Among these parameters, DOM has been considered to be the primary factor that influences membrane fouling (Gray *et al.* 2007). DOM in process water is a mixture containing soluble components and particulates with wide ranges of functional groups (hydroxyl, carboxylic acid, phenolic, and carbonyl groups) and molecular weights (MWs) (Logan and Jiang 1990). DOM can clog pores and block the surface of the membrane and reduce processing efficiency. To date, however, the fouling mechanisms of membranes and the influences of the physical and chemical properties of DOM, particularly the membrane operational conditions, have not been widely studied (Miyoshi *et al*. 2015; Wang *et al*. 2015).

In this study, according to its molecular weight, the DOM of process water was separated by ultrafiltration membranes into various fractions. DAX-8 and DAX-4 resins were used to identify the hydrophilicity of the fractions. The membrane fouling mechanism was elucidated by studying the filtration resistance and the linearized Herman's blocking models. The specific characteristics of DOM were investigated to determine the mechanism of membrane fouling.

EXPERIMENTAL

Papermaking Process Water Pretreatment

Papermaking process water was supplied by UPM, Changshu, Jiangsu, China. The process water was first pre-filtered with a 325-mesh filter cloth and a 0.45-μm pre-filter to remove large particulate material. The filter liquor (raw water) had TOC, 250 mg/L; pH, 8.10; electrical conductivity, 1783 μs/cm; and turbidity, 3.37 NTU.

Separation of DOM components

According to the technique suggested by Gray *et al.* (2004), various components of the DOM in raw water were separated using DAX-8 and DAX-4 resins. The raw water was fractionated into a strong hydrophobic fraction, which was Amberlite DAX-8-adsorbable; weakly hydrophobic fraction, which was retained on Amberlite DAX-4 resins; and a hydrophilic fraction that passed through both the DAX-8 and DAX-4 resins without adsorption (Ma *et al.* 2014). The strongly hydrophobic and weakly hydrophobic fractions were eluted using 0.1 M NaOH at 1 mL/min. The resins were initially washed with deionized water and methanol. The raw water was acidified to pH 2 before being fed into the resin column at 2 mL/min.

Molecular Weight (MW) Distribution

Pure nitrogen at a pressure of 0.1 MPa was used to drive the process water samples through polyethersulfone membranes with molecular weight cut-offs (MWCO) of 1, 5, 10, 30, and 100 kDa. The water samples were fractionated into portions of <1, 1 to 5, 5 to 10, 10 to 30, 30 to 100, and >100 kDa. These fractionation experiments were done in parallel, with identical initial samples fed to each membrane, rather than in a serial mode (Marieke *et al.* 2013). The contents of the various DOM components in raw water were characterized by TOC.

Membrane Filtration Operation

A stirred dead-end ultrafiltration (UF) module with an effective volume of 300 mL was used to evaluate the fouling properties of the membranes and the filterability of DOM components (Fig. 1). Polyethersulfone (PES) membranes were used in this study. The experimental apparatus was equipped with a stirrer that operated at a constant rate (250 rpm). The operating pressure was supplied by pure nitrogen at a constant 0.1 MPa. Before filtration, the ionic strength, Ca^{2+} content, and pH of all fractions were adjusted to the approximate values of raw process water using 1 M NaCl, 1 M CaCl$_2$, 1 M NaOH, and 1 M HCl. The filtrate was collected in a glass container placed on an electronic balance, and its mass was recorded every two minutes (Chen *et al.* 2007). The membrane flux was calculated from this data. In addition, the relative flux (J/J_0) was used to reduce error, where J (L/m^2·h) is the permeate flux and J_0 (L/m^2·h) is the pure water flux.
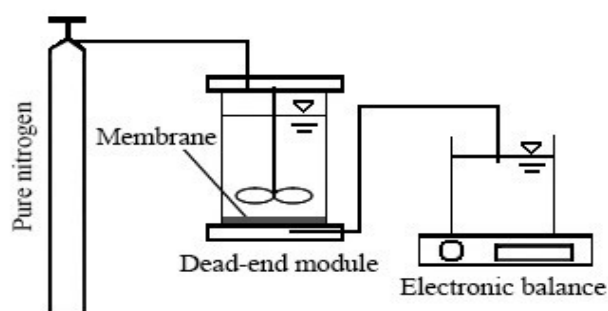

Fig. 1. Diagram of stirred dead-end ultrafiltration module

Scanning electron microscopy (SEM) and SEM-EDS analysis of membranes

The detailed structural information regarding the membranes was examined with scanning electron microscopy, using a filament voltage of 20 keV. Dry membrane samples were dispersed on a graphite ribbon fixed on an aluminum sample holder. The powders were sputter-coated with gold in a modular high-vacuum coating system Q150R ES (Quorum Technologies). The EDS was used to determine the inorganic foulants present in the membrane pores.

Analysis of Fouling Resistances

The fouling of a membrane is influenced by several factors, such as the formation of a cake layer, the concentration polarization on the membrane surface, and pore blocking. The distribution of different filtration resistances can be used to analyze the types of membrane fouling. In this study, the filtration resistances R_m (the intrinsic membrane resistance), R_a (the adsorption resistance), R_g (the pore blocking resistance), R_c (the cake resistance), and R_{cp} (the concentration polarization resistance) were measured. The filtration resistances were calculated using the following equations (Listiarini *et al.* 2009; Rajabi *et al.* 2015),

$$R_{\mathrm{m}} = \Delta P / \mu J_i \tag{1}$$

$$R_{\mathrm{a}} = \Delta P / \mu J_a - R_m \tag{2}$$

$$R_{\mathrm{g}} = \Delta P / \mu J_f - R_m - R_a \tag{3}$$

$$R_{\mathrm{c}} = \Delta P / \mu J_v - R_m - R_a - R_g \tag{4}$$

$$R_{\mathrm{cp}} = \Delta P / \mu J_l - R_m - R_c - R_g - R_a \tag{5}$$

where J_i is the pure water flux through a new membrane (L/m^2·h); J_a is the pure water flux through the membrane after static adsorbtion of organics from the process water (L/m^2·h); J_f is the pure water flux through the membrane, where surface contamination of the membrane adsorbed from process water was eliminated beforehand (L/m^2·h); J_v is the flux achieved at the end of ultrafiltration (L/m^2·h); J_l is the raw water flux through the membrane after static adsorbtion of organics from the process water (L/m^2·h); ΔP is the applied trans-membrane pressure (Pa); and μ is the viscosity of fresh water (Pa·s).

RESULTS AND DISCUSSION

Hydrophobicity and Molecular Weight Distribution

The results of the resin fractionation processes showed that DOM was mostly present in the form of hydrophilic components, which made up 68% of the total organic carbon in the process water. In addition, 14% of the DOM was strongly hydrophobic components, and approximately 18% was weakly hydrophobic components.
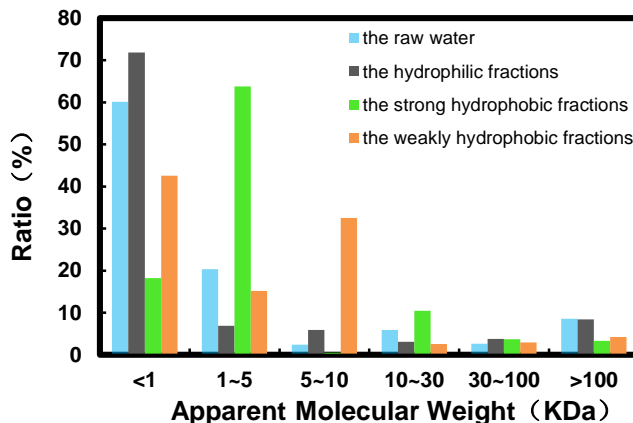
Fig. 2. MW distributions of various fractions

Table 1. Main Components of Carbohydrate in Raw Water Samples

RT (min)	Compound Name	Formula
5.647	arabinose	$C_5H_{10}O_5$
8.118	xylose	$C_5H_{10}O_5$
10.802	glucose	$C_6H_{12}O_6$
14.279	glucuronic acid	$C_6H_{10}O_7$
15.341	mannose	$C_6H_{12}O_6$
20.163	galacturonic acid	$C_6H_{10}O_7$
20.729	galactose	$C_6H_{12}O_6$

The results of the MW fractionation of DOM are shown in Fig. 2. For the raw water, the fraction with MW less than 1 kDa accounted for 60% of the total DOM. The 1 to 5 kDa fraction contributed about 20% of the total TOC. Fractions with MW larger than 5 kDa accounted for the lowest amount of the total TOC. The molecular weight distributions of the strongly hydrophobic, weakly hydrophobic, and hydrophilic fractions were similar to that of the raw water. The fractions with MW less than 5 kDa accounted for 82%, 58%, and 79% of the total DOM, respectively. The fractions with MW larger than 10 kDa accounted for only small percentages. During pre-filtering with a 0.45-µm filter, most

colloidal particles and large quantities of the high MW fractions were removed from the process water. This indicates that all fractions were dominated by DOM with MWs of less than 5 kDa.
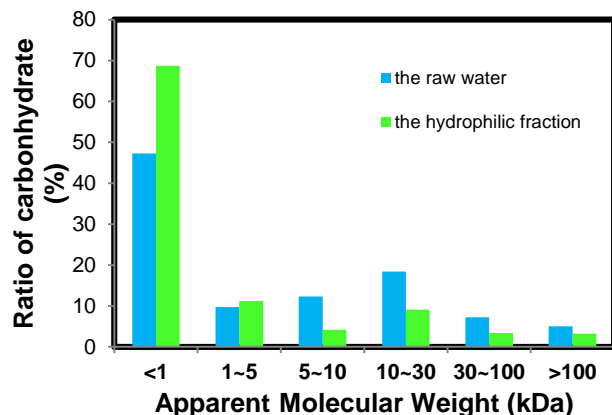

Fig. 3. Molecular weight distribution of carbohydrate results

Gas Chromatography-Mass Spectrometry (GC-MS) was used to characterize the components of carbohydrate in raw water. The water samples after methanolysis and silicon alkanisation were injected into the GC-MS apparatus (Agilent 6890/5793, USA, equipped with NIST05 mass spectral libraries). The injector temperature was 260 °C. The initial column temperature was 150 °C and was programmed to increase to 230 °C at a rate of 7 °C/min starting 0.5 min after injection. The detector temperature was 290 °C. The main components of carbohydrate in raw water are presented in Table 1. As shown in Table 1, components of carbohydrate in raw water are complex and mainly consisted of various saccharides and alduronic acid such as arabinose, xylose, glucose, mannose, galactose, and glucuronic acid.
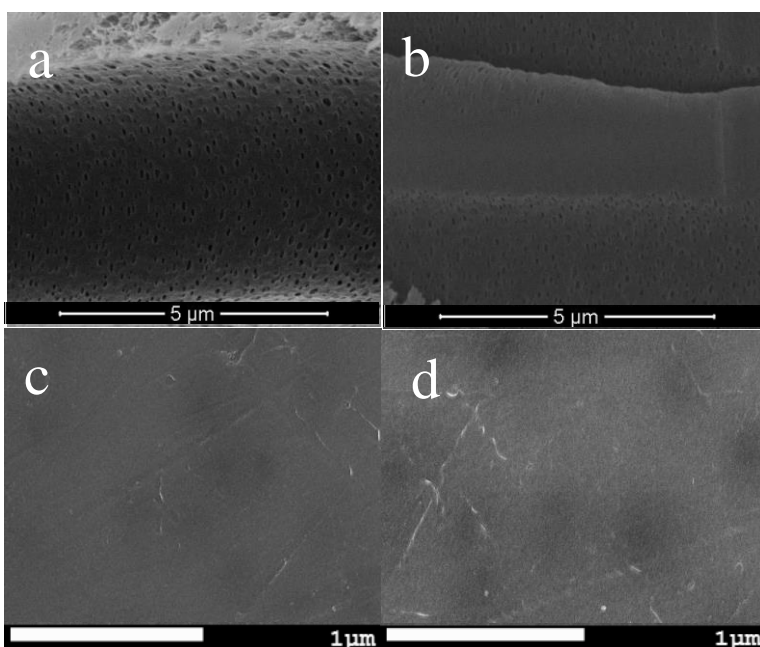

Fig. 4. SEM images of a) cross-section of pristine membrane; b) cross-section of membrane fed with the hydrophilic fractions; c) pristine membrane surface; d) fouled membrane surface fed with the hydrophilic fractions
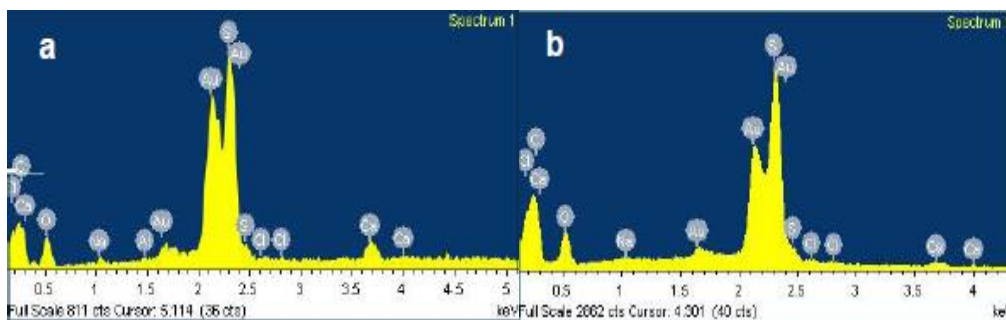
Fig. 5. EDS spectra of a) cross-section of pristine membrane; b) cross-section of fouled membrane

The carbohydrates in raw water mostly come from the degradation of cellulose, starch, and wood extractives (Chai *et al.* 2006; Huuha *et al.* 2010). The phenol–sulfuric acid method (Masuko *et al.* 2005) was designed to analyze the proportion of carbohydrate in fractions with different molecules weight. The results are shown in Fig. 3. As can be seen from Fig. 2 and Fig. 3, in terms of hydrophilic fraction, carbohydrate with MW less than 1 kDa accounted for 68.8% of the total carbohydrates. In contrast, carbohydrates with MW larger than 100 kDa accounted for only 3.3%. For the raw water, carbohydrates with MW less than 1 kDa accounted for 47.3% of the total carbohydrates. Carbohydrates with low molecular weight accounts for a large proportion, either in raw water or in the hydrophilic fraction. High concentrations of carbohydrates such as polysaccharides and monosaccharide contributes to the generally hydrophilic nature of DOM in whitewater (Huang *et al.* 2012).

Effects of DOM MW on Fouling Characteristics

The relative fluxes were plotted versus the filtration time to discuss the effect of the DOM's MW on the filtration behavior. UF using membranes with a MWCO of 30 kDa was performed to filter the six size components obtained previously. The ionic strength, Ca^{2+} content, and pH of all fractions were adjusted to the approximate values of raw water before filtration. Figure 6 shows the relative flux (J/J_0). The flux decline caused by DOM with MW less than 1 kDa was serious, reducing the flux by nearly 24% of its initial value. The slowest decline was caused by DOM with MW 10 to 30 kDa. It is generally believed that membrane fouling is dependent on several parameters, such as the source water's properties, solution chemistry, and membrane characteristics (Lee *et al.* 2006). In this case, the relationships between the membrane pore size and the size of the foulant have a great influence on the membrane flux (Ladner *et al.* 2010). DOM micromolecules may accumulate solutes on the membrane surface and form a gel layer or cake, reducing membrane permeability (Huang *et al.* 2007). The low-MW fractions can enter membrane pores, precipitate, and adsorb onto the pores' inner surfaces, altering the effective membrane porosity and causing irreversible fouling. When the low-MW DOM was filtered, pore blocking occurred quickly at the beginning of filtration. Pore narrowing seemed to affect the membrane flux more strongly. The cake formed on the membrane surface during filtering of high-MW DOM was considered to be loose and porous. According to the literature (Huang *et al.* 2012), large numbers of low MW DOM deposited on the membrane pore with a higher pore size. In other words, the results indicate that smaller contaminants are responsible for the fouling of large-pored membranes. In this

case, the membrane flux was less affected by macromolecular DOM, while the effect of small-molecule DOM on the membrane flux was more serious.

SEM images represented the changes between pristine and fouled membrane. As can be seen from Fig. 4a, there were many finger-like holes with homogeneous and compact pores inside the membrane. Most macromolecular colloids can be retained by these pores. The pristine membrane had a clean and smooth surface (Fig. 4c). After filtering low-MW fractions, the inside diameter of the holes visually decreased. The size of pores visible before ultrafiltration seemed to decrease, with some even disappearing as a result of pore blocking (Fig. 4b). Nevertheless, only a small amount of contaminant adhered to the membrane surface (Fig. 4d). An EDS analysis was performed to detect the elements present on the cross-sections of pristine and fouled membranes. As can be seen from Fig. 5, carbon, oxygen, and sulfur were the main elements detected in the pristine PES membrane pores. The contents of carbon and oxygen in the fouled membrane fed with the low-MW fractions increased. Large amounts of carbohydrates enter the membrane pores during ultrafiltration. In this case, the low-MW fractions tend to plug membrane pores.

Effects of DOM Hydrophobicity on Fouling Characteristics

To study the effects of the strongly hydrophobic, weakly hydrophobic, and hydrophilic fractions on membrane fouling, UF tests with the raw solution and the three fractions were carried out and compared. As is shown in Fig. 6, the hydrophilic fractions caused a higher fouling rate and greater flux decline than the other components. As shown in Fig. 7, the hydrophilic fractions caused the greatest decline in membrane flux, 58% of the initial flux in 50 min. The flux declines that resulted from the strongly hydrophobic and weakly hydrophobic fractions were only 29% and 40%, respectively. It is clear that the hydrophilic fraction was the major foulant in the DOM and was primarily responsible for the membrane flux decline. This result is well supported by the study of Zularisam (Zularisam *et al.* 2011).
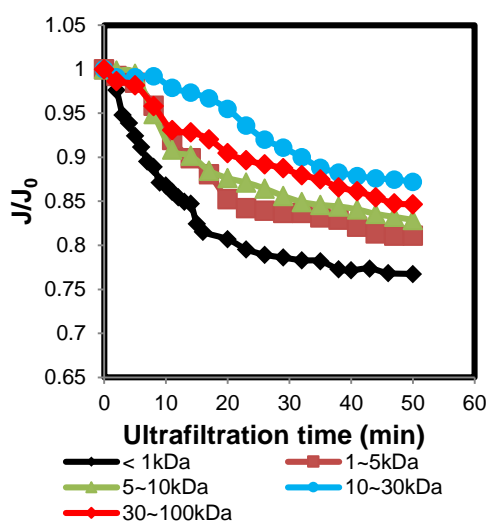

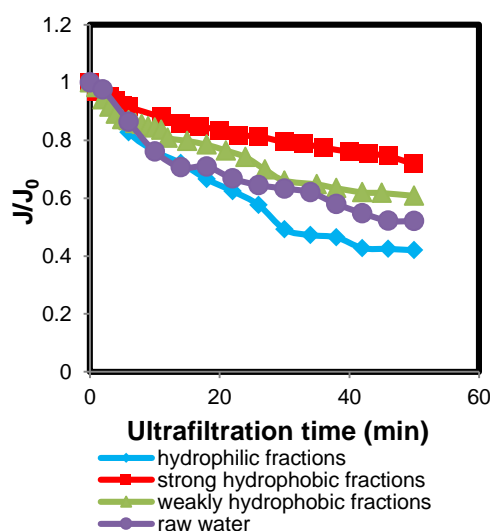**Fig. 6.** Decline in permeate flux for membranes with organics of various molecular weights

Fig. 7. Decline in permeate flux for membranes with hydrophilic/hydrophobic organics

The membrane flux decline caused by the DOM fractions was further studied through the fouling resistances. A close relationship between the DOM fractions and the filtration resistances was found. The hydrophilic fractions can quickly enter and block the membrane pores, decreasing membrane flux. This statement is supported by Fig. 8, which shows that the hydrophilic fractions had high R_g (18.25%). In addition, the filtration resistances of the strongly hydrophobic fractions showed that the cake layer and concentration polarization were the major fouling mechanisms causing its flux decline (Chang and Benjamin 2003). This statement is supported by the high values of R_{cp} (9.16%) and R_c (5.37%). Through analyzing the fouling resistance in DOM fractions filtration, it can be found that R_g in hydrophilic fractions was larger than that in hydrophobic fractions filtration, which resulted in the distinct decline of hydrophilic fractions flux. This phenomenon was maybe ascribed to the hydrophilic effect. That is, a very thin layer can be formed on the PES membrane surface by means of adsorption of hydrophobic fractions, while, more hydrophilic components tend to enter the inside of membrane pores, decreasing membrane flux (Domingues *et al*. 2014). Previous studies have indicated that organic fouling behavior in filtration depends on the chemical characteristics of feed and membrane properties (Chen *et al.* 2015; Chang *et al.* 2011). According to the various organic foulants on the membrane, the fouling caused by hydrophobic fractions is ascribed to the hydrophobic nature of PES membrane materials (Huang *et al.* 2012; Giglio 2013). Therefore, the hydrophobic fractions are prone to adhesion on the hydrophobic surface owing to the hydrophobic interaction.
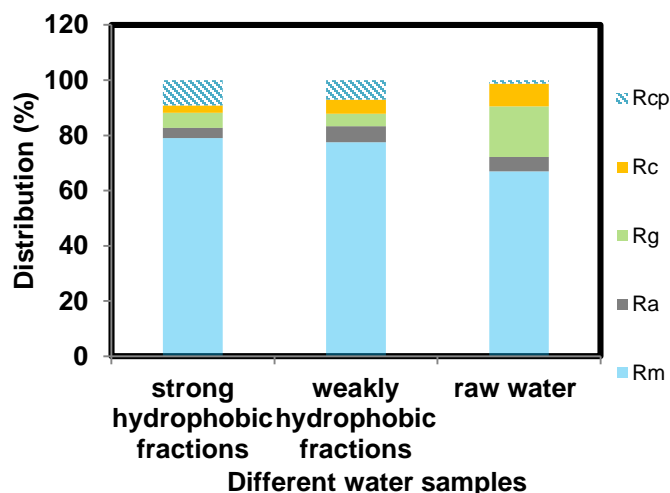

Fig. 8. Membrane resistances with hydrophilic/hydrophobic organics

Fouling Mechanism

To better understand the fouling mechanism of the PES membrane under the condition of dead-end filtration and constant pressure, the membrane flux *versus* filtration time curves were fitted using the constant pressure filtration blocking models (Hermia's semi-empirical model) listed in Table 1 (Vela *et al.* 2008; Mah *et al.* 2012; Wang *et al.* 2012). According to the modified Hermia model, there are four main fouling mechanisms: intermediate blocking; complete blocking; standard blocking; and gel layer formation.

Table 2. Constant Pressure Filtration Blocking Models

Blocking	Complete	Standard	Intermediate	Cake
Figure				
Model	$LnJ = LnJ_0 - K_1 t$	$1/J^2 = 1/J_0^{0.5} + 0.5 J_0^{0.5} K_2 t$	$1/J = 1/J_0 + K_3 t$	$1/J^2 = 1/J_0^2 + K_4 t / J_0$
Fitted Equation	$y = -K_1 x + b$	$y = 0.5 K_2 x + b$	$y = K_3 x + b$	$y = K_4 x + b$
y parameters	$y = LnJ$	$y = 1/(J \cdot J_0)^{0.5}$	$y = 1/J$	$y = J_0 / J^2$
b parameters	$b = LnJ_0$	$b = 1/J_0$	$b = 1/J_0$	$b = 1/J_0$
x parameters	$x = t$	$x = t$	$x = t$	$x = t$

Complete blocking occurs when the size of foulants is similar to the membrane pore size, which results in reducing the number of open pores without particle deposit on the membrane surface in the first place. Intermediate blocking is similar to complete blocking to some extent; a single particle can precipitate on other particles to form multi-layers, and it can directly block some membrane surfaces, resulting in an increase in cake thickness. Standard blocking is similar to adsorption, by which the particles approaching the membrane are adsorbed and deposited on the internal pore wall, thereby reducing the pore volume. The main fouling mechanism can be confirmed according to the relevant coefficients of determination (R^2) by calculating experimental data into these formulas. Larger R^2 values indicated better fitting models. The fitted situations and parameters of the models are shown in Figs. 9 to 12. According to the fitting results, the hydrophilic fractions can be appropriately approximated by the intermediate blocking model. The calculated coefficients of determination in this case were greater than 0.9824. The strongly hydrophobic and weakly hydrophobic fractions can be approximated by the cake blockage model. The calculated coefficients of determination were 0.9859 and 0.9839, respectively. This indicates that the strongly hydrophobic fractions caused the major cake layer and concentration polarization fouling, while intermediate blocking was primarily caused by the hydrophilic fractions. As shown in Fig. 2, great parts of hydrophilic fractions were low-MW organics that can enter membrane pores and precipitate onto their surfaces. In this case, pore narrowing and intermediate blocking played a significant part in membrane fouling, causing rapid declines in the membrane flux (Fellman *et al.* 2009; Goldman *et al.* 2012). Meanwhile, two factors were responsible for the hydrophobic fractions and the type of fouling mechanism. These factors are electrostatic repulsion and bridging action (Liang *et al.* 2007). Because of their phenolic and carboxylic moieties, the hydrophobic fractions were electronegative, resulting in electrostatic repulsion between organics and the PES membrane (Lisiarini *et al.* 2009). This repulsion prevented the hydrophobic fractions from adhering to the negatively charged surface of the membrane. In addition, the negatively charged surface of the membrane tended to bridge with the carboxylic groups of the hydrophobic fractions *via* calcium ions (Saravia *et al.* 2006), forming a cake layer on the membrane surface. The cake layer could be alleviated to some extent by the stirrer, whereas the blocking within pores of the membrane caused by the hydrophilic fractions was irreversible. It was observed that such internal blocking and pore narrowing caused by the hydrophilic fractions were the main factors that led to the membrane fouling.
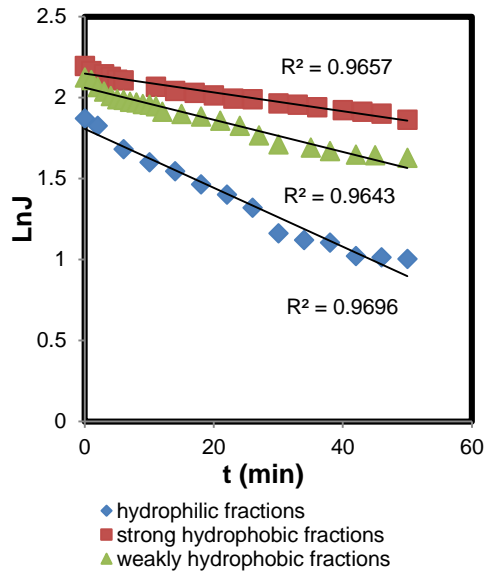
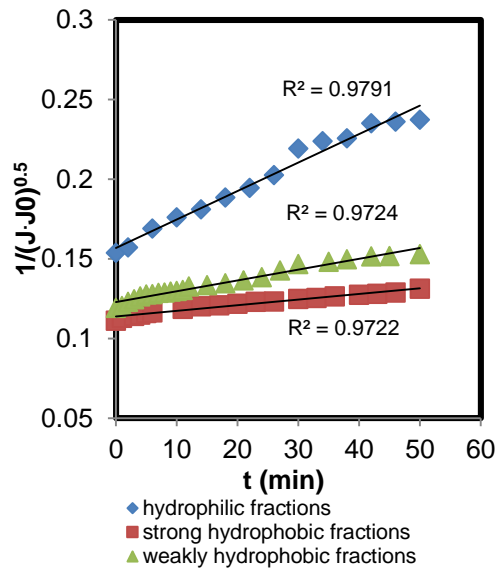**Fig. 9.** The complete blocking model fitting of hydrophilic/hydrophobic organics

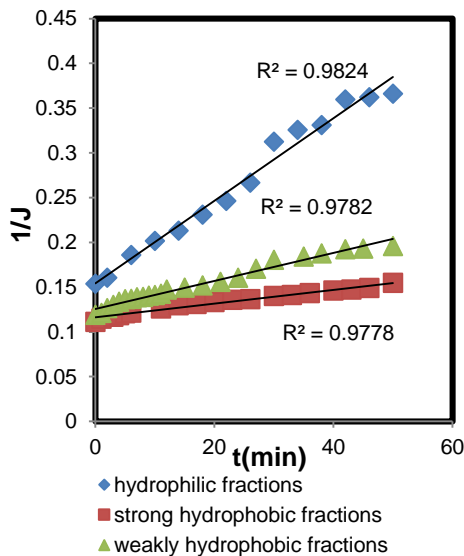**Fig. 10.** The standard blocking model fitting of hydrophilic/hydrophobic organics

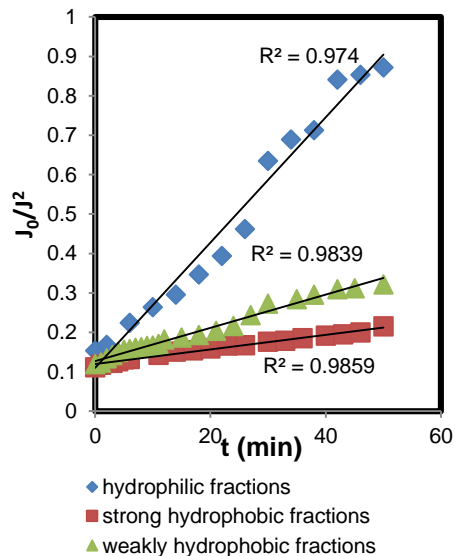**Fig. 11.** The intermediate blocking model fitting of hydrophilic/hydrophobic organics

Fig. 12. The cake blockage model fitting of hydrophilic/hydrophobic organics

CONCLUSIONS

1. The results of the resin fractionation processes showed that the dissolved organic matter (DOM) was mostly present in the form of hydrophilic components, which made up 68% of the total organic carbon in the paper machine whitewater. The results of the MW fractionation of DOM showed that fractions with MW less than 5 kDa accounted for up to 80% of the TOC.

2. Studying the effects of the DOM MW on the fouling characteristics showed that DOM micromolecules may accumulate solutes on the membrane surface and form gel layers

or a cake, causing membrane fouling. The low-MW fractions may enter the membrane pores and adsorb onto their inner surface, causing irreversible fouling. Compared to the DOM micromolecules, low-MW fractions contributed more to membrane fouling.

3. The filtration resistance and linearized Herman's blocking models showed that hydrophobic fractions exhibited a cake layer and concentration as the major fouling mechanisms, while the intermediate blocking was primarily caused by the hydrophilic fractions. Cake layer formation and pore plugging were the main mechanisms of membrane fouling by the DOM. The hydrophilic fraction was the major foulant causing the membrane flux to decline.

ACKNOWLEDGMENTS

REFERENCES CITED

Carroll, T., King, S., and Gray, S. R. (2000). "The fouling of microfiltration ion membrane by NOM after coagulation treatment," *Water Research* 34(11), 2861-2868. DOI: 10.1016/S0043-1354(00)00051-8

Chai, X. S., Samp, J. C., Yang, Q. F., Song, H. N., Zhang, D. C., and Zhu, J. Y. (2006). "Determination of microstickies in recycled whitewater by headspace gas chromatography," *Journal of Chromatography A* 1108(1), 14-19. DOI: 10.1016/j.chroma.2005.12.108

Chang, E. E., Yang, S. Y., Huang, C. P., Liang, C. H., and Chiang, P. C. (2011). "Assessing the fouling mechanisms of high-pressure nanofiltration membrane using the modified Hermia model and the resistance-in-series model," *Separation and Purification Technology* 79(3), 329-336. DOI: 10.1016/j.seppur.2011.03.017

Chang, Y. J., and Benjamin, M. M. (2003). "Modeling formation of natural organic matter fouling layers on ultrafiltration membranes," *Journal of Environmental Engineering-ASCE* 129(1), 25-32. DOI: 10.1061/(ASCE)0733-9372(2003)129:1(25)

Chen, Y., Dong, B. Z., Gao, N. Y., and Fan, J. C. (2007). "Effect of coagulation pretreatment on fouling of an ultrafiltration membrane," *Desalination* 204(1-3), 181-188. DOI: 10.1016/j.desal.2006.04.029

Chen, X. G., Luo, J. Q., Qi, B. K., Cao, W. F., and Wan, Y. H. (2015). "NOM fouling behavior during ultrafiltration: Effect of membrane hydrophilicity," *Journal of Water Process Engineering* 7, 1-10. DOI: 10.1016/j.jwpe.2015.04.009

Chen, X. Q., Shen, W. H., Kou, S. L., and Liu, H. B. (2011). "GC-MS study of the removal of dissolved and colloidal substances in recycled papermaking by flocculation with nano-size TiO_2 colloids," *BioResources* 6(3), 3300-3312. DOI: 10.15376/biores.6.3.3300-3312

Choi, B. G., Cho, J., Song, K. G., and Maeng, S. K. (2013). "Correlation between effluent organic matter characteristics and membrane fouling in a membrane bioreactor using

advanced organic matter characterization tools," *Desalination* 309(1), 74-83. DOI: 10.1016/j.desal.2012.09.018

Domingues, R. C. C., Ramos, A. A., Cardoso, V. L., and Reis, M. H. M. (2014). "Microfiltration of passion fruit juice using hollow fibre membranes and evaluation of fouling mechanisms," *Journal of Food Engineering* 121, 73-79. DOI: 10.1016/j.jfoodeng.2013.07.037

Fellman, J. B., Miller, M. P., Cory, R. M., D'Amore, D. V., and White, D. (2009). "Characterizing dissolved organic matter using PARAFAC modeling of fluorescence spectroscopy: A comparison of two models," *Environmental Science & Technology* 43(16), 6228-6234. DOI: 10.1021/es900143g

Giglio, F. (2013). "The use of materials from biomass as construction materials," *Open Journal of Civil Engineering* 3(2A), 82-84. DOI: 10.4236/ojce.2013.32A009

Goldman, J. H., Rounds, S. A., and Needoba, J. A. (2012). "Applications of fluorescence spectroscopy for predicting percent wastewater in an urban stream," *Environmental Science & Technology* 46(8), 4374-4381. DOI: 10.1021/es2041114

Gray, S. R., Ritchie, C. B., and Bolto, B. A. (2004). "Effect of fractionated NOM on low pressure membrane flux declines," *Natural Organic Material Research: Innovations and Applications for Drinking Water* 4(4), 189-196.

Gray, S. R., Ritchie, C. B., Tran, T., and Bolto, B. A. (2007). "Effect of NOM characteristics and membrane type on microfiltration performance," *Water Research* 41(17), 3833-3841. DOI: 10.1016/j.watres.2007.06.020

Huang, H., Lee, N., Young, T., Amy, G., Lozier, J. C., and Jacangelo, J. G. (2007). "Natural organic matter fouling of low-pressure, hollow fiber membranes: Effects of NOM source and hydrodynamic conditions," *Water Research* 41(17), 3823-3832. DOI: 10.1016/j.watres.2007.05.036

Huang, Y. Z., Huang, T. H., Yang, J. H., and Damodar, R. A. (2012). "Identifications and characterizations of proteins from fouled membrane surfaces of different materials," *International Biodeterioration & Biodegradation* 66(1), 47-52. DOI: 10.1016/j.ibiod.2011.09.009

Huuha, T. S., Kurniawah, T. A., Sillanpaa, M. E. T. (2010). "Removal of silicon from pulping whitewater using integrated treatment of chemical precipitation and evaporation," *Chemical Engineering Journal* 158(3), 584-592. DOI: 10.1016/j.cej.2010.01.058

Huuhilo, T., Suvilumpi, J., and Puro, L. (2002). "Internal treatment of pulp and paper mill process waters with a high temperature aerobic biofilm process combined with ultrafiltration and/ or nanofiltration," *Paperi ja Puu-Paper and Timber* 84(1), 50-53.

Kilduff, J. E., and Mattaraj, S. (2004). "Flux decline during nanofiltration of naturally-occurring dissolved organic matter effects of osmotic pressure, membrane permeability, and cake formation," *Journal of Membrane Science* 239(1), 39-53. DOI: 10.1016/j.memsci.2003.12.030

Ladner, D. A., Vardon, D. R., and Clark, M. M. (2010). "Effects of shear on microfiltration and ultrafiltration fouling by marine bloom forming algae," *Journal of Membrane Science* 356(1-2), 33-43. DOI: 10.1016/j.memsci.2010.03.024

Lee, N., Amy, G., Croue, J. P., and Philippe, J. (2006). "Low-pressure membrane fouling associated with allochthonous and autochthonous natural organic matter," *Water Research* 40(12), 2357-2368. DOI: 10.1016/j.watres.2006.04.023

Lee, S., Choi, J. S., and Lee, C. H. (2009). "Behaviors of dissolved organic matter in membrane desalination," *Desalination* 238(1-3), 109-116. DOI: 10.1016/j.desal.2008.01.041

Liang, S., Liu, C., and Song, L. (2007). "Soluble microbial products in membrane bioreactor operation: behaviors, characteristics, and fouling potential," *Water Research* 41(1), 95-101. DOI: 10.1016/j.watres.2006.10.008

Lisiarini, K., Chun, W., Sun, D. D., and Leckie, J. O. (2009). "Fouling mechanism and resistance analyses of systems containing sodium alginate, calcium, alum and their combination in dead-end fouling of nanofiltration membranes," *Journal of Membrane Science* 344(1-2), 244-251. DOI: 10.1016/j.memsci.2009.08.010

Listiarini, K., Sun, D. D., and Leckie, J. O. (2009). "Organic fouling of nanofiltration membranes: Evaluating the effects of humic acid, calcium, alum coagulant and their combinations on the specific cake resistance," *Journal of Membrane Science* 332(1-2), 56-62. DOI: 10.1016/j.memsci.2009.01.037

Logan, B., and Jiang, Q. (1990). "Molecular-size distributions of dissolved organic-matter," *Journal of Environmental Engineering-ASCE* 116(6), 1046-1062. DOI: 10.1061/(ASCE)0733-9372(1990)116:6(1046)

Lowe, J., and Hossain, M. M. (2008). "Application of ultrafiltration membranes for removal of humic acid from drinking water," *Desalination* 218(1-3), 343-354. DOI: 10.1016/j.desal.2007.02.030

Ma, D. F., Peng, B., Zhang, Y. H., Gao, B. Y. Wang, Y., Yue, Q. Y., and Li, Q. (2014). "Influence of dissolved organic matter characteristics on trihalomethanes formation during chlorine disinfection of membrane bioreactor effluents," *Bioresource Technology* 165(S1), 81-87. DOI: 10.1016/j.biortech.2014.02.126

Mah, S. K., Chuah, C. K., Lee, W. P. C., and Chai, S. P. (2012). "Ultrafiltration of palm oil-oleic acid-glycerin solutions: Fouling mechanism identification, fouling mechanism analysis and membrane characterizations," *Separation and Purification Technology* 98(19), 419-431. DOI: 10.1016/j.seppur.2012.07.020

Marieke, V. A., Stephane, P., and Genevieve, G. G. (2013). "Ultrafiltration membrane cut-off impacts structure and functional of transmitted proteins: Case study of the metalloprotein α-lactalbumin," *Separation and Purification Technology* 114(8), 73-82. DOI: 10.1016/j.seppur.2013.04.038

Masuko, T., Minami, A., Lwasaki, N., Majima, T., Nishimura, S., and Lee, Y. C. (2005). "Carbohydrate analysis by a phenol-sulfuric acid method in microplate format," *Analytical Biochemistry* 339(1), 69-72. DOI: 10.1016/j.ab.2004.12.001

Miyoshi, T., Yamamura, H., Morita, T., and Watanabe, Y. (2015). "Effect of intensive membrane aeration and membrane flux on membrane fouling in submerged membrane bioreactors: Reducing specific air demand per permeate (SAD_p)," *Separation and Purification Technology* 148(25), 1-9. DOI: 10.1016/j.seppur.2015.04.030

Natalia, G. O., Paloma, H. H., Raquel, D. G., Manuel, A. S., Antonio, M. P., and Pilar, B. B. (2013). "Evaluation of tangential flow ultrafiltration procedures to assess trace metals bound to marine dissolved organic matter," *Microchemical Journal* 110(10), 501-509. DOI: 10.1016/j.microc.2013.06.004

Rajabi, H., Ghaemi, N., Madaeni, S., Daraei, P., Astinchap, B., Zinadini, S., and Razavizadeh, S. H. (2015). "Nano-ZnO embedded mixed matrix polyethersulfone (PES) membrane: Influence of nanofiller shape on characterization and fouling

resistance," *Applied Surface Science* 349(15), 66-77. DOI: 10.1016/j.apsusc.2015.04.214

Rocas, L., Collado, S., and Gutierrez, A. (2014). "Fouling mechanisms of *Pseudomonas putida* on PES microfiltration membranes," *Journal of Membrane Science* 465(1), 27-33. DOI: 10.1016/j.mernsci.2014.04.002

Saravia, F., Zwiener, C., and Frimmel, F. H. (2006). "Interactions between membrane surface, dissolved organic substances and ions in submerged membrane filtration," *Desalination* 192(1-3), 280-287. DOI: 10.1016/j.desa1.2005.07.039

Stevenson, S. (1990). "With a zero-effluent mill Millar Western will meet the stringent Saskatchewan standards," *Pulp and Paper-Canada* 91(1), 16-18.

Vela, M. C. V., and Blanco, S. A. (2008). "Analysis of membrane pore blocking models applied to the ultrafiltration of PEG," *Separation and Purification Technology* 62(3), 489-498. DOI: 10.1016/j.seppur.2008.02.028

Wang, C. X., Li, Q., Tang, Q., Yan, D. J., Zhou, W., Xing, J. X., Wan, Y. H. (2012). "Membrane fouling mechanism in ultrafiltration of succinic acid fermentation broth," *Bioresource Technology* 116, 366-371. DOI: 10.1016/j.biortech.2012.03.099

Wang, J., Yang, J., Zhang, H. W., Guo, W. S., and Ngo, H. H. (2015). "Feasibility study on magnetic enhanced flocculation for mitigating membrane fouling," *Journal of Industrial and Engineering Chemistry* 26(25), 37-45. DOI: 10.1016/j.jiec.2014.11.038

Wu, X. B., Xie, Y. M., and Yang, H. T. (2009). "Application of the physico-chemical process to the advanced treatment of paper-making white wastewater," *Industrial Water Treatment* 29(2), 41-43.

Wu, R., He, B., Zhang, B., Zhao, G. L., Li, J. R., and Li, X. F. (2014a). "Preparation of immobilized pectinase on regenerated cellulose beads for removing anionic trash in whitewater from papermaking," *Journal of Chemical Technology and Biotechnology* 89(7), 1103-1109. DOI: 10.1002/jctb.4223

Wu, R., He, B., Zhao, G. L., and Li, X. F. (2014b). "Immobilization of pectinase on polyethyleneimine-coated pulp fiber for treatment of whitewater from papermaking," *Journal of Molecular Catalysis B: Enzymatic* 99(2), 163-168. DOI: 10.1016/j.molcatb.2013.11.007

Zularisam, A. W., Ahmad, A., Sakinnah, M., and Ismail, A. F. (2011). "Role of natural organic matter (NOM), colloidal particles, and solution chemistry on ultrafiltration performance," *Separation and Purification Technology* 78(2), 189-200. DOI: 10.1016/j.seppur.2011.02.001